Carbohydrate Polymers **21** (1993) 99–104

'B' to 'A' type phase transition in short amylose chains

P. Le Bail, H. Bizot & A. Buléon

Laboratoire de Physicochimie des Macromolécules, INRA, BP 527, 44026 Nantes Cedex 03, France

For short amylose chains (DP 15), the solid state transition from the hexagonal B to monoclinic A crystalline type was detected by X-ray powder diffraction and differential scanning calorimetry (DSC). It occured on the minute time scale in the range 20–40% H_2O dry basis (d.b.) for temperatures around 130–90°C, whereas similar 'Heat Moisture Treatments' of Sair, L. (1967, *Cereal Chem.*, **40**, 8) required hours with native maize starch granules at 20% H_2O d.b.

INTRODUCTION

Natural and processed starches (mixtures of linear and branched poly α(1-4) anhydroglucoses) occur under various (partially) crystalline types defined by their X-ray powder diffractograms. The corresponding structures result from different helical conformations and packing arrangements. The A-type is usually found in cereal starches, the B-type is mostly characteristic of tubers in amylose-rich starches and the C-types are considered as mixtures of the former. The different V-types are obtained after complexing with various guest,s bearing some analogy with cyclodextrins (French, 1984, Biliaderis, 1992). In contrast with cellulosic materials, the apparent crystallinity as revealed by diffraction techniques depends on the hydration level (Buleon *et al.*, 1982). Its qualitative and quantitative control is relevant to raw material production (drying and storage) as well as industrial processing (pasting, melting and complexing) or biological availability (digestion and degradation) (Colonna *et al.*, 1992).

Addressing the question of determining phase diagrams of water–starch systems requires better definition of the following:

(1) the polymeric composition of the samples, i.e. the chain lengths, the number and regularity of branching and the fractions of minor components (lipids, ions, etc.);
(2) the architecture of the semi-crystalline mixtures produced by biosynthesis (granules), by water dispersion and recrystallisation (gels or precipitates) followed by subsequent hydrolysis and/or drying, or by organic solvent dissolution and precipitation;
(3) the state of hydration of the mixtures;
(4) the recognition of the non-equilibrium (metastable) character of most aqueous starch–water systems (Biliaderis, 1992) where most processes are under kinetic control (Slade & Levine, 1991), particularly those involving the nucleation and propagation of the two main structural features of polyanhydroglucose chains, i.e. the helicity and the inter-chain packing.

Under reduced water contents, say below 50% H_2O dry basis (d.b.), multiple melting endotherms have been observed by differential scanning calorimetry (DSC) of native granular starches of potato (Donavan, 1979; Donavan *et al.*, 1983; Tomka, 1991) or rice (Biliaderis, 1990). Using short linear chains we attempt here to clarify the conditions leading to one of the polymorphic interconversions as mentioned in the literature for natural starches, i.e.:

(1) A-type to B-type conversion as observed after gelatinisation (irreversible swelling and dispersion) and retrogradation (partial recrystallisation) of native granules heated above 60°C in excess (extragranular) water as for gel ageing or bread staling;
(2) B-type to A-type after 'heat moisture treatments' such as those proposed by Sair (Sair & Fetzer, 1944; Sair, 1964, 1967) for maize starches tempered at 100°C and 20% H_2O d.b. for 18 h.

Carbohydrate Polymers 0144-8617/93/$06.00

From the proposed structures available in the literature (Wu & Sarko, 1978*a,b*; Imberty *et al.*, 1987, 1991; Imberty & Perez, 1988), the main difference between A- and B-types arises from the less dense packing of double helices in the B-type. These accommodate a water column replacing an amylose double helix surrounded by six other double helices as part of the hexagonal lattice, which results in a structure more prone to annealing effects than the monoclinic lattice of A-type amylose.

After a brief description of short chain preparation by hydrochloric acid hydrolysis, the combination of differential scanning calorimetry and X-ray powder diffractometry is used to detect and identify the various transitions occurring during sequential heat treatments of a crystalline B-type substrate at various levels of hydration.

EXPERIMENTAL

Sample preparation

Mild acid hydrolysis

Short linear chains of crystalline amylose of B-type (average degree of polymerisation DP = 15 glucose units) were obtained as the residual fractions of controlled acid hydrolysis (litnerisation) of native potato starch granules, following the procedure of Robin *et al.* (1975). After hydrolysis in 2·2N hydrochloric acid for 35 days at 35°C, the residual fraction (25% of initial weight) was thoroughly washed and centrifuged in distilled water to reach neutral pH. Instead of freeze drying (Muhr *et al.*, 1984), subsequent drying was obtained by solvent exchanges following the sequence ethanol/acetone/ethyl-ether. In our case, the original crystalline type is retained, while synthetic crystals of short amylose chains may be obtained in either A or B form depending on crystallisation condition (Buleon *et al.*, 1984).

Water sorption conditioning

Grounded powders were brought to various water contents following the isopiestic water vapour (ad- and de-)sorption procedure essentially similar to the COST 90 recommendations (Jowitt & Wagstaffe, 1989). The water contents were determined on aliquots after drying, first to 50°C for 0·5 h followed by 130°C for 1·5 h. Salts for saturated salt solutions were of analytical grade.

DSC measurement

An automated heat flux 'differential scanning calorimeter' (SETARAM DSC III, France) was used for the thermal analysis of 100 mg samples sealed in stainless steel high pressure cells. Most scans between 20 and 180°C were run at 3°C/min and ±40 mW full scale. Calibration was checked on indium (429·6 K) and gallium (302·7 K) melting. The reference cell contained dry alumina powder.

Following the heat treatments (usually in the calorimeter) the pressure cells were quenched in liquid nitrogen, warmed up to room temperature, wiped dry and cut open, and the ground products were reconditioned to 75% relative vapour pressure to reach a water content suitalbe for higher quality X-ray diffractograms.

X-ray diffraction measurements

The crystalline type was determined by transmission Wide Angle X-Ray Scattering (WAXS) on powders using the CuKα_1 radiation (λ = 0·154 05 nm), with a tube voltage of 40 kV and a tube current of 30 mA. A 120° (2θ) curved detector (CPS 120, INEL, France) was used to monitor the diffracted intensities during 1 h exposure periods. Zinc oxide was used for calibrations.

Samples of about 40 mg were compacted as 1 mm by 6 mm diameter discs and covered by 0·01 mm aluminium foil to prevent evaporation during the measurement.

RESULTS AND DISCUSSION

Calorimetry

In this paper, we focus mainly on structurally identified transistors. Similar thermograms were obtained irrespective of the ad- or desorption state, in agreement with the fact that the amplitude of sorption hysteresis decreases rapidly as the temperature rises. The thermograms are sensitive to water content; most endotherms rise to higher temperatures as the water content decreases, but they may also disappear; examples are given in Fig. 1. Concerning the intensity of structural disruption by acid hydrolysis, sulphuric acid treatments (Nageli) have traditionally led to weaker modifications of the enthalpy and temperature of gelatinisation (Donovan & Mapes, 1980) than hydrochloric acid attacks (Muhr *et al.*, 1984). The decrease of the gelatinisation enthalpy and the concurrent minor rise of transition temperature may finally vanish at lower moisture concentration. A minimum of 50% H_2O (d.b.) and more than one α(1-6)-branch point per chain have been considered as prerequisite to observe well-defined interactions (Blanshard, 1987). However, a low temperature endotherm of weak amplitude is systematically observed in the range 50–64°C as the moisture content drops from 25 to 4% H_2O (d.b.) (Table 1). This endotherm (I in Fig. 1) will subsequently be called the *'restoration'* peak in analogy to *'rejuvenation'* phenomena observed on physically aged amorphous polymers which display enthalpy relaxation. Similar patterns

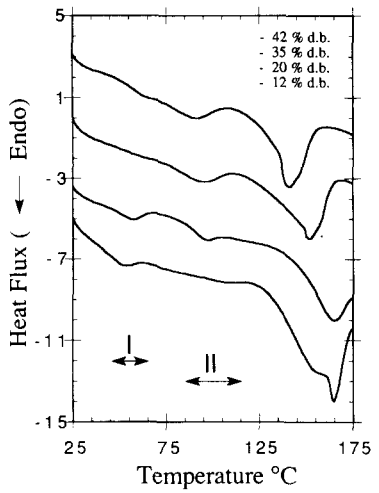

Fig. 1. Characteristic thermal profiles of potato starch lintners (DP 15) at various water contents (from bottom to top: 11·5, 20·4, 35·5 and 42·5% H_2O (d.b.).

were detected on amorphous powders of amylopectin (Kalichevsky *et al.*, 1992) or starch (Shogren, 1992), and systematically identified in very different types of low moisture powders of polysaccharides (Gidley *et al.*, 1992). A detailed discussion of such patterns will appear elsewhere. Presently we would attribute this effect to the evolution of those amorphous local patches of the hydrated lintner, which may physically age (modify their configuration by slow diffusion processes) in an efficient manner (i.e. have their local glass transition temperature about 25° above the average room temperature (Ten Brinke *et al.*, 1989)). We thus speculate that polysaccharide powders may behave like mixtures of polymers with varying sensitivity to plasticisation by water.

Above 20% H_2O (d.b.), an interesting phenomenon (II in Fig. 1) preceding the main melting endotherm was detected in the case of B-type DP15 potato lintner (but not on similar A-type lintners: data not shown), at temperatures steadily decreasing from 100°C as the water content rises. In order to identify the structural origin of this peak, sequential heat treatments, interrupted at successively increasing temperatures, were conducted in the calorimeter. Subsequent X-ray diffraction measurements were performed on the corresponding samples after moisture content adjustment. As will be shown, this peak apparently corresponds to a polymorphic phase transition involving a change in the packing of helices. The energies involved in this type of lattice disruption are generally small, here 1 to 4 J/g between 20 and 40% H_2O (d.b.). For comparison, the transition from free to crystalline helical V-type amylose complexes, i.e. the packing energy, is about 0·7 J/g (Biliaderis, 1990; Whittam *et al.*, 1990), while the energy of gelatinisation may amount to about 10 to 20 J/g for native starches. Concerning crystallisation, the propagation state is known to be a much less limiting factor than nucleation as the polymer chain length decreases, as shown for amylose solutions of DP 170 and 2000 (Kitamura & Kuge, 1989). We may thus expect that structural changes concomitant with heat moisture treatments may take place during the heating ramp of the DSC, leading to conditions for our short chains comparable to those developed by longer processes on native granules (Lorentz & Kulp, 1982, 1983). Moreover Shogren (1992), studying low moisture corn starch, has identified an exothermal valley separating two endotherms attributed to amylopectin 'melting' in the temperature range 140–180°C and hydration from 30 to 15% H_2O wet basis (w.b.). This is reminiscent of recrystallisation phenomena following melting or devitrification, but no structural method was employed to correlate this finding to a definite mechanism. Generally speaking, the enthalpy measured represents the balance between endothermic swelling and/or melting and exothermic effects such as hydration. In this respect, the loss of long range order and the amylose-amylopectin interactions are not directly related to the magnitude of the gelatinisation enthalpy. If the Flory plots determined for Nageli amylodextrins (Donovan & Mapes, 1980) or synthetic DP 15 spherocrystals (Whittam *et al.*, 1990) are *extrapolated* at lower

Table 1. Enthalpies and maximum peak temperatures of main endotherms obtained by DSC at 3°C/min on hydrated DP 15 B-type starch lintners

% H_2O (d.b.)	4%	5%	7%	9%	11%	14%	17%	18%	20%	23%	29%	35%	42%
T_1 (°C)	63·4	62·4	63·4	60·9	58·9	58·9	55·8	50·6	50·6	50·6	62·2		62·3
ΔH_1 (J/g)	−0·4	−0·5	−0·6	−1·2	−1·2	−1·2	−1·4	−2·2	−1·7	−1·6	−0·8		−0·5
T_2 (°C)									100	102·3	98·2	92·6	88·6
ΔH_2 (J/g)									?	−0·2	−1.2	−2·7	−4·0
T_3 (°C)				164·9	162·8	155/170	140/170	150/165	168·3	166·1	154·3	152·5	141·1
ΔH_3 (J/g)	(*)[a]	(*)	(*)	(*)	(*)	(*)	(*)	(*)	(*)	−13·6	−19·1	−19·6	−20·4

[a](*) Incomplete or bimodal endotherms.

hydrations, the A- or B-type short chains may be expected to melt at around 150–170°C. From this latter study, a temperature difference of 15 to 20° is noted between the more stable A and the B-type (peak temperatures should rise from 140°C to 180°C as moisture content drops from 35 to 15% H_2O (d.b.)). In this range, the order of magnitude of 'melting' enthalpies reaches about 20 J/g while the spherocrystals were reported to have values similar for both types, i.e. 35 J/g (Whittam *et al.*, 1990; Noel & Ring, 1992) or 42 J/g for DP 22 (Ring *et al.*, 1987). Even if insufficient hydration hampers melting, our lower enthalpy values probably indicate the partial crystallinity of directly obtained lintners and leave room for some phenomena taking place in the amorphous fraction such as *'restoration'*.

In our case, below 20% H_2O (d.b.), the second endotherm II (80–100°C) was no longer observed, while the main melting (150–180°C) frequently appeared as bimodal. The lower temperature drift of the maximum with water content may be connected to a B- to A-type interconversion. This remains to be proven by in-situ spectroscopy. The details of the melting process of *cationic* potato starch granules have been investigated in the range 10–20% H_2O (w.b.) at 10°C/min (Tomka, 1991; Willenbucher *et al.*, 1992). Using a complementary structural method, it was shown that following the gelatinisation transition (50–80°C) the melting process displays a double peak in the range 100–175°C. A two-step mechanism was proposed by these authors. The disappearance of X-ray crystallinity (fragmentation of large crystallites) would be followed by the loss of backbone helicity as measured by ^{13}C CP/MAS NMR spectroscopy; the overlapping of the two processes suggests that the system relaxes in the course of the transformation. Surprisingly, the low moisture samples molten above 120°C but below 165–200°C are able to recrystallise ('retrograde') into the A-type. In our case we may expect less connectivity between short amylose chains than in native granules; however, the second part of the melting endotherm is characterized by a sharp front which suggests high cooperativity. More precise investigations are planned with intermediate chain lengths. Above 170° or 180°C the risks of degradation preclude further investigation (Gidley & Bulpin, 1987; Tomasik *et al.*, 1989), particularly at our moderate heating rate (3°C/min).

Glass transition patterns

Heat capacity step changes were apparently detected during the second DSC run, following the first temperature scan for samples containing 4 to 8% H_2O (d.b.). The low apparent glass transition temperatures (inflection points) detected in these conditions were around 60 to 30°C, but partial degradation during the first scan could not be excluded (browning and irreproducibilities appearing before any detectable change in the IR spectra). In comparison to the studies of Orford *et al.* (1989) on malto-oligosaccharides, the T_g values expected should not differ much from malto-oligomer values which are about 60–100°C in this water content range.

X-ray diffraction

Structural signatures of starches (Buleon *et al.*, 1990) are characterised by specific diffraction peaks observed at 2θ Bragg angles:

— A-type: 9·9, 11·2, 15, 17, 18·1 and 23·3°
— B-type: 5·6, 15, 17, 22 and 24°

Typically the apparent crystallinity (sharpness and intensity of peaks relative to the amorphous background) increases steadily with hydration up to at least 35% H_2O (d.b.) (Cleven *et al.*, 1978; Buleon *et al.*, 1982, 1987). The peaks at 5·6° (possibly related to interhelical distance) and 24° are particularly sensitive in this respect. To ease our observations heat treatments were followed by quenching and rehydration to water contents around 15% H_2O (d.b.) assuming negligible evolution of products at room temperature.

Above 20% H_2O (d.b.), two potato starch lintners have been specifically studied at 35 and 42% H_2O (d.b.), the intercrystalline phase transition B- to A-type having been identified in the temperature range 90–110°C, following the appearance of the second endotherm close to 90°C (Fig. 2). The primary structural change to be detected was the disappearance of the 5·6° peak above 65°C (data not shown); subsequently the 17° peak split to produce a second maximum at 18·1°, and the two peaks at 22 and 24° merged to one sharp

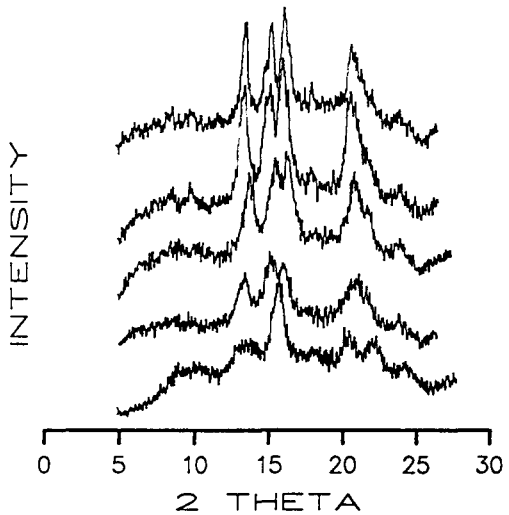

Fig. 2. Evolution of WAXS spectra for originally B-type lintners (35% H_2O (d.b.)) with increasing maximum temperature of heat treatment (from bottom to top: 60°C 'B-type', 100°C 'Biphasic A+B', 112°C 'A-type', 135°C 'Annealed A-type', 152°C 'Perfected A-type').

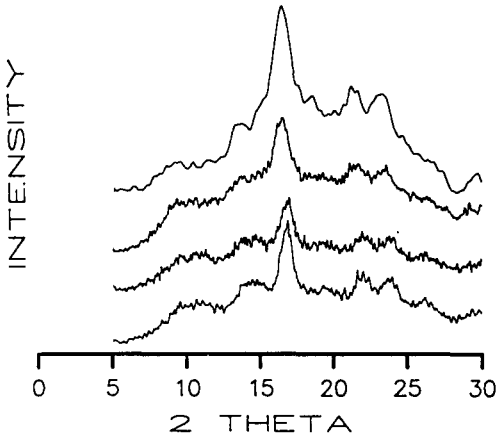

Fig. 3. Evolution of WAXS spectra for originally B-type lintners (12% H_2O (d.b.)) with increasing maximum temperature of heat treatment. (from bottom to top: 57, 77, 100 and 125°C).

peak at 23·3°. As the temperature of the heat treatment exceeded 130°C a neat A-type pattern was obtained. Further perfectioning of the structure could probably occur after appropriate annealing around the transition temperature, instead of heating at 3°C/min. In our case, the solid-solid phase transition was not associated with an obvious exotherm, as was suggested in the results of Shogren (1992). Below 20% H_2O (d.b.), as shown in Fig. 3, no evolution of X-ray patterns could be detected for heat treatments before degradation of our products appeared.

Closer investigations of bimodal peaks, following the findings of Willenbucher *et al.* (1992), and possibly attempts to increase the heating kinetics and planned. Other authors have observed thermograms where multiple endotherms pointing to recrystallisation or solid state phase conversion may explain the transitions in varying conditions of molecular weight, concentration and kinetics (crystalline nucleation/propagation and melting as influenced by heating/cooling rates). Supplemental information to construct an amylose/water phase diagram (or state diagram; Slade & Levine, 1991) may soon be available on the thermodynamic level for intermediate chain lengths, such as DP 41 (Leloup *et al.*, 1990), diluted along amylose chains (Doublier *et al.*, 1992) or aged molten starches (Shogren, 1992).

CONCLUSIONS

In addition to the numerous discussions concerning structural changes in amylosic materials upon hydrothermal treatments, the main point of this work was to delimit the B-type to A-type phase change of short chain amylose (DP 15) in the range 20–40% H_2O (d.b.) between 90 and 130°C.

The diversity in conditions calls for numerous experiments before delineating the precise borders and pathways for polymorphic phase transitions of glucans, and structural methods have to be coupled to thermodynamic measurements to clarify the situation.

The revival of older works connected with the 'heat moisture treatments' of Sair & Fetzer (1944), then related to the technology of dextrin production, is motivated by the understanding of the melting phenomena during the extrusion of low moisture products (Tomka, 1991) as well as the chain-chain associations leading to gel or precipitate formation (Doublier *et al.*, 1992) or resistant starch production during baking (Rabe & Sievert, 1992).

REFERENCES

Biliaderis, C.G. (1990). In *Thermal Analysis of Foods*, ed. V.R. Harwalkar & C.Y. Ma, Elsevier, New York, pp. 168–220.

Biliaderis, C.G. (1992). *Food Technol.*, **46**(6), 98–145.

Blanshard, J.M.V. (1987). In *Starch: Properties and Potential; Critical Reports on Applied Chemistry*, ed. T. Gaillard. John Wiley & Sons, New York, **13**, 16–54.

Buleon, A., Bizot, H., Delage, M.M. & Multon, J.L. (1982). *Starch/Stärke*, **34**, 361.

Buleon, A., Duprat, F., BOoy, F.P. & Chanzy, H. (1984). *Carbohydr. Polym.*, **4**, 161–73.

Buleon, A., Bizot, H., Delage, M.M. & Pontoire, B. (1987). *Carbohydr. Polym.*, **7**, 461–82.

Buleon, A., Colonna, P. & Leloup, V. (1990). *Ind. Aliment. Agr.*, **6**, 515–32.

Cleven, R., Van der Plas, L. (1978). *Starch/Stärke*, **30**, 233–8.

Colonna, P., Leloup, V. & Buleon, A. (1992). *Eur. J. Clin. Nutr.*, **46**, S17–S32.

Donavan, J.W. (1979). *Biopolymers*, **18**, 263–75.

Donavan, J.W. & Mapes, C.J. (1980). *Starch/Stärke*, **32**, 190–3.

Donavan, J.W., Lorentz, K. & Kulp, K. (1983). *Cereal. Chem.*, **60**, 381–7.

Doublier, J.L., Coté, I., Llamas, G. & Charlet, G. (1992). *Prog. Colloid Polym. Sci.*, **90**, 61–5.

French, D. (1984). In *Starch: Chemistry and Technology*, ed. R.L. Whistler, E.F. Panshall & J.N. Bemiller, Academic Press, New York, pp. 183–247.

Gidley, M.J. & Bulpin, P.V. (1987). *Carbohydr. Res.*, **161**, 291–300.

Gidley, M.J., Cooke, D. & Ward-Smith, S. (1992). In *Proceedings of 'The Science and Technology of the Glassy State in Foods'*, ed. J.M.V. Blanshard & P.J. Lillford, Nottingham University, 6–9 April.

Imberty, A. & Perez, S. (1988). *Biopolymers*, **22**, 341–6.

Imberty, A., Chanzy, H., Perez, S., Buleon, A. & Tran, V. (1987). *Food Hydrocolloids*, **1**, 455–9.

Imberty, A., Buleon, A., Tran, V. & Perez, S. (1991). *Starch/Stärke*, **43**, 375–84.

Jowitt, R. & Wagstaffe, P.J. (1989). *BCR Information: Reference Materials*, EUR 12429 EN, pp. 1–54.

Kalichevsky, M.T., Jaroszkiewicz, E.M., Ablett, S. & Blanshard, J.M.V. (1992). *Carbohydr. Polym.*, **18**, 77–88.

Kitamura, S. & Kuge, T. (1989). *Food Hydrocolloids*, **3**, 313–26.

Leloup, V.M., Colonna, P. & Ring, S. (1990). *Macromolecules*, **23**, 862–6.

Lorentz, K. & Kulp, K. (1982). *Starch/Stärke*, **34**, 50–4.

Lorentz, K. & Kulp, K. (1983). *Starch/Stärke*, **35**, 123–9.
Muhr, A.H., Blanshard, J.M.V. & Bates, D.R. (1984). *Carbohydr. Polym.*, **4**, 399–425.
Noel, T.R. & Ring, S.G. (1992). *Carbohydr. Res.*, **227**, 203–13.
Orford, P.D., Parker, R. & Ring, S.G. (1989). *Carbohydr. Res.*, **196**, 11–18.
Rabe, E. & Sievert, D. (1992). *Eur. J. Clin. Nutr.*, **46**, Suppl. 2, 105–7.
Ring, S.G., Miles, M.J., Morris, V.J., Turner, R. & Colonna, P. (1987). *Int. J. Biol. Macromol.*, **9**, 158–60.
Robin, J.P., Mercier, C., Duprat, F., Charbonnière, R. & Guilbot, A. (1975). *Starch/Stärke*, **27**, 36–44.
Sair, L. (1964). In *Methods of Carbohydrate Chemistry*, Vol. 4, ed. R.L. Whistler, Academic Press, New York, p. 283.
Sair, L. (1967). *Cereal. Chem.*, **40**, 8.
Sair, L. & Fetzer, W.R. (1944). *Ind. Eng. Chem.*, **36**, 205.
Shogren, R.L. (1992). *Carbohydr. Polym.*, **19**, 83–90.
Slade, L. & Levine, H. (1991). *Critical Reviews in Food Science and Nutrition*, **30**, 115–360.
Ten Brinke, G. & Grooten, R. (1989). *Macromolecules*, **16**, 244–9.
Tomasik, P., Wiejak, S. & Pakasinski, M. (1989). *Advances in Carbohydrate Chemistry and Biochemistry*, **47**, 279–344.
Tomka, I. (1991). In *Water Relationships in Foods. Advances in the 1980s and Trends for the 1990s*, ed. H. Levine & L. Slade, Plenum Press, New York, pp. 627–37.
Whittam, M.A., Noel, T.R. & Ring, S.G. (1990). *Int. J. Biol. Macromol.*, **12**, 359–62.
Willenbucher, R.W., Tomka, I. & Muller, R. (1992). *Zucker-industrie*, **1**, 49–62.
Wu, H.C. & Sarko, T. (1978*a*). *Carbohydr. Res.*, **61**, 7–26.
Wu, H.C. & Sarko, T. (1978*b*). *Carbohydr. Res.*, **61**, 27–40.